

# Constraining Vectorlike Quark Model from B Radiative Decays

XIONG Zhao-Hua<sup>1)</sup>

(Theoretical Physics Group, College of Applied Science, Beijing University of Technology, Beijing 100022, China)

**Abstract** In the  $SU(2)$  singlet down type vectorlike quark model, there exist a tree level coupling  $z_{sb}$  of  $b \rightarrow sZ^*$  and an additional D quark. In the framework we evaluate the D quark effects on  $B \rightarrow X_s \gamma$  by running the Wilson coefficients of the effective Hamiltonian with the renormalization scale from  $m_D$  to weak scale. Using the recent measurements for  $B \rightarrow X_s l^+ l^-$ , we extract rather stringent constraints on the size and CP violating phase of  $z_{sb}$ , and find that the zero point of the forward-backward asymmetry may have large deviation from that of the standard model and is very sensitive to  $z_{sb}$ , and therefore, it can be useful in probing the new physics.

**Key words** B radiative decays, tree level coupling of  $bsZ$ , vectorlike quark model

## 1 Introduction

The rare radiative decays  $B \rightarrow X_s \gamma$  and  $B \rightarrow X_s l^+ l^-$  are sensitive probes of new physics<sup>[1]</sup>. Unlike in the standard model (SM) where flavor changing neutral currents (FCNC) arise only at loop level, in the vector quark model (VQM)<sup>[2, 3]</sup>, the CKM matrix is necessarily non-unitarity, leading to interaction  $Z\bar{s}b$  at tree level, and hence potentially large new physics contributions can be expected.

There are some studies regarding the constraints on model with extra singlet quark<sup>[2, 3]</sup>. In this work, (i) we first integrate out the heavy D quark. New operators are introduced for  $b \rightarrow s\gamma$ ; (ii) since vectorlike down-type quark contributions to  $b \rightarrow s\gamma$  just occur at loop level as the case of the SM, the constraints from  $B \rightarrow X_s \gamma$  on  $z_{sb}$ , the tree level FCNC coupling for  $b \rightarrow sZ$ , are less restrictive compared to those from those processes governed by  $b \rightarrow sl^+ l^-$  transition. Recently, the rare decays  $B \rightarrow X_s l^+ l^-$  ( $l = e, \mu$ ) also have been measured by BaBar and Belle<sup>[4, 5]</sup>. In light of the improvements mentioned above, it is necessary to present a comprehensive analysis in this model.

## 2 $b \rightarrow s\gamma$ and $b \rightarrow sl^+ l^-$ transitions in vectorlike quark model

In VQM the difference between the new quark and ordinary quarks of the three SM generations is that both the left- and right-handed components of the former quark are  $SU(2)$  singlets, leading to non-unitarity as

$$z_{\alpha\beta} \equiv \sum_{i=1}^3 V^{\alpha i} V^{\beta i*} = \sum_{i=1}^3 V_{\text{CKM}}^{i\alpha*} V_{\text{CKM}}^{i\beta} = \delta_{\alpha\beta} - V^{\alpha 4} V^{\beta 4*}, \quad (1)$$

where the matrix  $V_{\text{CKM}}$  is enlarged to  $3 \times 4$  and  $V$  is a  $4 \times 4$  unitary matrix which relates the weak-eigenstates  $\bar{q}_L$  to mass-eigenstates  $q_L$ . The deviations from the standard unitary triangles are going to vanish as the down type singlet mass increases compared with electroweak breaking scale  $v$ . The relevant interaction Lagrangian can be found in Ref. [2].

In VQM, the down-type vector quark may be much heavier than weak scale. In a theory with different mass scales, the heavier scale should be integrated out firstly, then Wilson coefficients are run with the

Received 15 August 2005, Revised 26 October 2005

1) E-mail: xiongzhang@mail.ihep.ac.cn

renormalization scale from heavier scale to low scale by using renormalization group equation. Only when  $m_D$  is about the weak scale, can W, Z boson, Higgs boson and top quark be integrated out together. In this work, we consider two possibilities as follows:

Scenario A:  $m_W^2 \ll m_D^2$

By keeping only the leading order terms of  $\delta_D = m_W^2/m_D^2$ , we obtain the effective Hamiltonian for  $b \rightarrow s\gamma^*(g^*)$  as:

$$\mathcal{H}_{\text{eff}}^{\text{new}}[b \rightarrow \gamma^*(g^*)] = \frac{4G_F}{\sqrt{2}} z_{4s}^* z_{4b} \sum_i C_i(\mu) \mathcal{O}_i(\mu). \quad (2)$$

A complete basis for the local operators is listed below<sup>1)</sup>:

$$\begin{aligned} \mathcal{O}_{\text{LR}}^1 &= -\frac{1}{16\pi^2} m_b \bar{s}_L \mathcal{D}^2 b_R, \\ \mathcal{O}_{\text{LR}}^2 &= \frac{1}{16\pi^2} g_s m_b \bar{s}_L \sigma^{\mu\nu} T^a b_R G_{\mu\nu}, \\ \mathcal{O}_{\text{LR}}^3 &= \frac{1}{16\pi^2} e e_d m_b \bar{s}_L \sigma^{\mu\nu} b_R F_{\mu\nu}, \\ Q_{\text{LR}}^{\phi^0} &= \frac{1}{2} g_s^2 m_b \phi^0 \phi^0 \bar{s}_L b_R, \\ P_L^{1,A} &= -i \frac{1}{16\pi^2} \bar{s}_L T_{\mu\nu\sigma}^A \mathcal{D}^\mu \mathcal{D}^\nu \mathcal{D}^\sigma b_R, \\ P_L^2 &= \frac{1}{16\pi^2} \bar{s}_L \gamma^\mu b_R \partial^\nu F_{\mu\nu}, \\ R_L^{1,\phi^0} &= i \frac{1}{2} g_s^2 \phi^0 \phi^0 \bar{s}_L \not{D} b_L, \\ R_L^{2,\phi^0} &= i g_s^2 (\partial^\sigma \phi^0) \phi^0 \bar{s}_L \gamma_\sigma b_L, \end{aligned} \quad (3)$$

where  $T^a$  stands for the  $SU(3)_{\text{color}}$  generator,  $F_{\mu\nu}$  and  $G_{\mu\nu}$  are field strengths of photon and gluon respectively.  $\mathcal{D}_\mu = \partial_\mu - i g_s G_\mu^a T^a - i e e_d A_\mu$  is the covariant derivative.  $\phi^0 = H^0$ ,  $G^0$ , and  $G^0$  stands for Goldstone boson. The tensors  $T_{\mu\nu\sigma}^A$  ( $A = 1, 2, 3, 4$ ) appearing in  $P_L^{1,A}$  have the following Lorentz structures<sup>[6]</sup>:

$$\begin{aligned} T_{\mu\nu\sigma}^1 &= g_{\mu\nu} \gamma_\sigma, & T_{\mu\nu\sigma}^2 &= g_{\mu\sigma} \gamma_\nu, \\ T_{\mu\nu\sigma}^3 &= g_{\nu\sigma} \gamma_\mu, & T_{\mu\nu\sigma}^4 &= -i \epsilon_{\mu\nu\sigma\tau} \gamma^\tau \gamma_5. \end{aligned} \quad (4)$$

The coefficients of operators  $Q_{\text{LR}}$  and  $R_L$  at scale  $m_D$  can be obtained by matching the diagrams of full theory with effective theory at tree level while for those of  $\mathcal{O}_{\text{LR}}$ ,  $P_L$ , by matching one loop diagrams shown in Fig. 1. They read

$$C_{Q_{\text{LR}}^{\text{H}^0}}(m_D) = -C_{Q_{\text{LR}}^{\phi^0}}(m_D) = -\frac{1}{g_s^2},$$

$$\begin{aligned} C_{R_L^{1,\phi^0}}(m_D) &= 2C_{R_L^{2,\phi^0}}(m_D) = -\frac{1}{2g_s^2}, \\ C_{O_{\text{LR}}^i}(m_D) &= 0, \quad C_{P_L^{1,1}}(m_D) = C_{P_L^{1,3}}(m_D) = -\frac{11}{18}, \\ C_{P_L^{1,2}}(m_D) &= \frac{8}{9}, \quad C_{P_L^{1,4}}(m_D) = -\frac{1}{2}, \quad C_{P_L^2}(m_D) = 0, \end{aligned} \quad (5)$$

where  $i$  runs from 1 to 3. The values for operators  $O$ ,  $P$  are understood as the sum of  $H^0$  and  $G^0$  contributions.

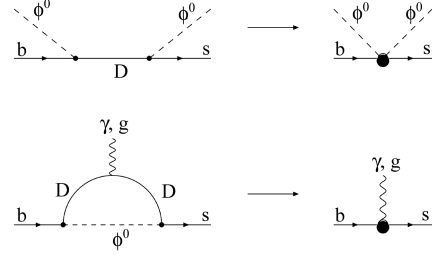


Fig. 1. Matching conditions at scale  $m_D$  in full theory (left) and in the intermediate effective field theory (right). Note that  $\phi^0$  in the second line of diagrams is not integrated out yet.

To obtain the coefficients of the operators at weak scale, we extract the anomalous dimensions by calculating one-loop diagrams in unitary gauge with operator insertions. Then we solve renormalization group equation (RGE) and have the coefficients at  $m_W$  scale as follows:

$$\begin{aligned} C_{O_{\text{LR}}^1} &= \frac{247}{548} \zeta^{-\frac{4}{21}} + \frac{336}{8905} \zeta^{\frac{113}{126}} - \frac{511}{780} \zeta^{\frac{8}{21}} + \frac{1}{6} \zeta^{\frac{2}{3}}, \\ C_{O_{\text{LR}}^2} &= \frac{247}{1096} \zeta^{-\frac{4}{21}} + \frac{168}{8905} \zeta^{\frac{113}{126}} - \frac{223}{780} \zeta^{\frac{8}{21}} + \frac{1}{24} \zeta^{\frac{2}{3}}, \\ C_{O_{\text{LR}}^3} &= \frac{247}{1096} \zeta^{-\frac{4}{21}} + \frac{168}{8905} \zeta^{\frac{113}{126}} - \frac{223}{780} \zeta^{\frac{8}{21}} + \frac{5}{12} \zeta^{\frac{2}{3}} - \frac{3}{8} \zeta^{\frac{16}{21}}, \\ C_{P_L^{1,1}} &= C_{P_L^{1,3}} = -\frac{247}{548} \zeta^{-\frac{4}{21}} - \frac{791}{4932} \zeta^{\frac{113}{126}}, \\ C_{P_L^{1,2}} &= \frac{247}{548} \zeta^{-\frac{4}{21}} + \frac{1}{12} \zeta^{\frac{8}{21}} + \frac{875}{2466} \zeta^{\frac{113}{63}}, \\ C_{P_L^{1,4}} &= -\frac{247}{598} \zeta^{-\frac{8}{21}} - \frac{1}{12} \zeta^{\frac{8}{21}} + \frac{14}{411} \zeta^{\frac{113}{126}}, \\ C_{P_L^2} &= 0, \end{aligned} \quad (6)$$

where  $\zeta = \alpha_s(m_D)/\alpha_s(m_W)$ .

To match the operator set in (3) onto these operators obtained by integrating out the W, Z bosons, Goldstone boson, Higgs boson and top quark as in SM, we use the equations of motion to reduce all the

1)Strictly speaking,  $\phi^0$  in Fig. 1 can be  $Z^0$  boson, which indicates that there exists operator  $Z_\mu Z^\mu \bar{s}_R b_L$ . However, since its coefficient is suppressed by large scale  $m_D$ , its contribution can be neglected safely in Scenario A

remaining two-quark operators to the gluon and photon magnetic moment operators  $\mathcal{O}_{\text{LR}}^2$  and  $\mathcal{O}_{\text{LR}}^3$  which are redefined as  $\mathcal{Q}_{\text{8G}}$  and  $\mathcal{Q}_{\text{7}\gamma}$ . Now the effective Hamiltonian describing  $b \rightarrow sl^{+1-}$  transition reads<sup>[7]</sup>

$$\mathcal{H}_{\text{eff}} = -\frac{4G_{\text{F}}}{\sqrt{2}}K_{\text{tb}}K_{\text{ts}}^* \left[ \sum_{i=1}^{10} \tilde{C}_i(\mu)\mathcal{Q}_i(\mu) + \tilde{C}_{\text{7}\gamma}(\mu)\mathcal{Q}_{\text{7}\gamma}(\mu) + \tilde{C}_{\text{8G}}(\mu)\mathcal{Q}_{\text{8G}}(\mu) + \mathcal{C}_9(\mu)\mathcal{O}_9(\mu) + \mathcal{C}_{10}(\mu)\mathcal{O}_{10}(\mu) \right], \quad (7)$$

where  $\mathcal{Q}_i$  ( $i=1-10$ ) are four-quark operators,  $K_{ij} \equiv (V_{\text{CKM}})_{ij}$  for  $i, j=1, 2, 3$ .

Now we rewrite the Wilson coefficients as  $C = C^{\text{SM}} + C^{\text{new}}$  where  $C^{\text{SM}}$  stands for that of SM<sup>[7]</sup> while  $C^{\text{new}}$  denotes the deviation of the values between VQM and SM. After straightforward calculations, at  $m_{\text{W}}$  scale, we have non-vanishing coefficients for new physics contributions:

$$\begin{aligned} \tilde{C}_2^{\text{new}} &= -\kappa, & \tilde{C}_3(m_{\text{W}}) &= -\frac{1}{6}\kappa, \\ \tilde{C}_7^{\text{new}} &= -\frac{2}{3}\sin^2\theta_{\text{W}}\kappa, & \tilde{C}_9^{\text{new}} &= -\frac{2}{3}\cos^2\theta_{\text{W}}\kappa, \\ \tilde{C}_{\text{7}\gamma}^{\text{new}} &= \left[ \frac{23}{36} - \frac{1}{4}e_{\text{d}} \left( C_{\text{O}_{\text{LR}}^1} - 4C_{\text{O}_{\text{LR}}^3} + C_{\text{P}_{\text{L}}^{1,1}} + C_{\text{P}_{\text{L}}^{1,2}} - C_{\text{P}_{\text{L}}^{1,4}} \right) + e_{\text{d}} \left( \frac{1}{3} + \frac{1}{9}\sin^2\theta_{\text{W}} \right) \right] \kappa, \\ \tilde{C}_{\text{8G}}^{\text{new}} &= \left[ \frac{1}{3} - \frac{3}{4}e_{\text{d}} \left( C_{\text{O}_{\text{LR}}^1} - 4C_{\text{O}_{\text{LR}}^3} + C_{\text{P}_{\text{L}}^{1,1}} + C_{\text{P}_{\text{L}}^{1,2}} - C_{\text{P}_{\text{L}}^{1,4}} \right) - 3e_{\text{d}} \left( \frac{1}{3} + \frac{1}{9}\sin^2\theta_{\text{W}} \right) \right] \kappa, \\ \mathcal{C}_9^{\text{new}} &= \frac{\pi}{\alpha_{\text{em}}}\kappa(-1+4\sin^2\theta_{\text{W}}), & \mathcal{C}_{10}^{\text{new}} &= \frac{\pi}{\alpha_{\text{em}}}\kappa, \end{aligned} \quad (8)$$

where  $\kappa \equiv \frac{z_{\text{sb}}}{K_{\text{tb}}K_{\text{ts}}^*}$ . In deriving the above equation, we have used the unitarity relation  $z_{4b}z_{4s}^* = -z_{\text{sb}}$  which is a direct result of Eq. (1).

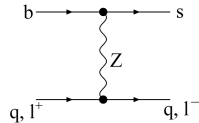


Fig. 2. Tree level Feynman diagram contributing to  $b \rightarrow sy$  and  $b \rightarrow sl^{+1-}$ .

At this moment, we would like to point out that these new contributions have different sources. The terms proportional to  $\frac{z_{\text{sb}}}{K_{\text{tb}}K_{\text{ts}}^*}$  in  $\tilde{C}_{3,7,9}$  and  $\mathcal{C}_{9,10}$  come from the tree-level diagram as displayed in Fig. 2 whereas in  $\tilde{C}_2$ , from tree diagram due to the non-

unitarity of CKM matrix in VQM<sup>[2]</sup>. In expressions of  $\tilde{C}_{\text{7}\gamma, \text{8G}}$ , the first constant term comes from the charged current one-loop diagrams due to the non-unitarity of CKM matrix in VQM, other terms proportional to  $\frac{z_{\text{sb}}}{K_{\text{tb}}K_{\text{ts}}^*}$  come from the neutral current one-loop diagrams.

Scenario B:  $m_{\text{W}}^2 \sim m_{\text{D}}^2$

In this scenario, the t and D quark, W and Z can be integrated out together. The corresponding initial values of Wilson coefficients  $\tilde{C}_{\text{7}\gamma, \text{8G}}(m_{\text{W}})$  are changed to<sup>[2]</sup>

$$\begin{aligned} \tilde{C}_{\text{7}\gamma}^{\text{new}} &= \left[ \frac{23}{36} + (f_{\text{D}}^{\text{Z}}(y_{\text{D}}) + f_{\text{D}}^{\text{H}}(w_{\text{D}}) + f_{\text{D}}^{\text{G}}(y_{\text{D}})) + e_{\text{d}} \left( \frac{1}{3} + \frac{1}{9}\sin^2\theta_{\text{W}} \right) \right] \kappa, \\ \tilde{C}_{\text{8G}}^{\text{new}} &= \left[ \frac{1}{3} - 3(f_{\text{D}}^{\text{Z}}(y_{\text{D}}) + f_{\text{D}}^{\text{H}}(w_{\text{D}}) + f_{\text{D}}^{\text{G}}(y_{\text{D}})) - 3e_{\text{d}} \left( \frac{1}{3} + \frac{1}{9}\sin^2\theta_{\text{W}} \right) \right] \kappa, \end{aligned} \quad (9)$$

where  $y_{\text{D}} = m_{\text{D}}^2/m_{\text{Z}}^2$ ,  $w_{\text{D}} = m_{\text{D}}^2/m_{\text{H}}^2$ . Other Wilson coefficients are the same as Scenario A we discussed. The function  $f_y^x$  stands for the contribution from boson x mediated penguin one-loop diagram with quark y in loops. They have forms as

$$\begin{aligned} f_{\text{D}}^{\text{Z}}(x) &= -\frac{5x^2 + 5x - 4}{72(x-1)^3} + \frac{x(2x-1)}{12(x-1)^4} \ln x, \\ f_{\text{D}}^{\text{H}}(x) &= -e_{\text{d}}x \left[ \frac{7x^2 - 29x + 16}{48(x-1)^3} + \frac{3x-2}{8(x-1)^4} \ln x \right], \\ f_{\text{D}}^{\text{G}}(x) &= e_{\text{d}}x \left[ \frac{5x^2 - 19x + 20}{48(x-1)^3} + \frac{x-2}{8(x-1)^4} \ln x \right]. \end{aligned} \quad (10)$$

As a consistency check, in Scenario B in limit of  $m_{\text{D}} \gg m_{\text{W}}$ , from Eqs. (9), (10) one can infer that the term  $f_{\text{D}}^{\text{Z}}(y_{\text{D}}) + f_{\text{D}}^{\text{H}}(w_{\text{D}}) + f_{\text{D}}^{\text{G}}(y_{\text{D}}) \rightarrow \frac{1}{24}e_{\text{d}}$ , which is the value of the term  $-\frac{1}{4}e_{\text{d}}[C_{\text{O}_{\text{LR}}^1} - 4C_{\text{O}_{\text{LR}}^3} + C_{\text{P}_{\text{L}}^{1,1}} + C_{\text{P}_{\text{L}}^{1,2}} - C_{\text{P}_{\text{L}}^{1,4}}]$  in (8) if the QCD running of the coefficients with the renormalization scale from  $m_{\text{D}}$  to  $m_{\text{W}}$  is negligible. Therefore, under the approximation, values of  $\tilde{C}_{\text{7}\gamma}(m_{\text{W}})$  and  $\tilde{C}_{\text{8G}}(m_{\text{W}})$  in Scenario A would be equivalent to those in Scenario B. Our calculation also shows that the running effect on the parts from neutral current in Scenario A is large; however, at  $m_{\text{W}}$  scale, since the new dominant contribution comes from the charged current diagrams, the total

values of  $\tilde{C}_{\gamma, sG}(m_W)$  are changed slightly. Since the coefficients are insensitive to the mass of  $m_D$ , in the follows we will focus on Scenario A and study how to constrain the interaction coupling of Z FCNC  $z_{sb}$  in VQM using B radiative decays.

### 3 Constraints on $z_{sb}$ in VQM from $B \rightarrow X_s l^+ l^-$

Now we constrain the parameter  $z_{sb}$  from  $B \rightarrow X_s l^+ l^-$ . The invariant dilepton distribution is

$$\frac{d\Gamma(B \rightarrow X_s l^+ l^-)}{ds} = \left(\frac{\alpha_{em}}{4\pi}\right)^2 \frac{G_F^2 m_b^5 |K_{ts}^* K_{tb}|^2}{48\pi^3} (1-s) R_0,$$

$$R_0 = 4 \left(1 + \frac{2}{s}\right) |\tilde{C}_{\gamma}^{eff}|^2 + (1+2s) (|\mathcal{C}_9^{eff}|^2 + |\mathcal{C}_{10}^{eff}|^2) + 12\text{Re}(\tilde{C}_{\gamma}^{eff} \mathcal{C}_9^{eff*}). \quad (11)$$

It depends on the tree level FCNC coupling  $z_{sb}$  and  $|K_{tb} K_{ts}|$  which is determined by

$$|K_{tb} K_{ts}^*| \simeq |K_{cb} K_{cs}^*| + |z_{sb}| \cos \theta, \quad \theta = \arg(\kappa), \quad (12)$$

where  $|K_{cb} K_{cs}|$  can be used as input of the direct experimental values<sup>[8]</sup>.

There is some progress in predicting  $B \rightarrow X_s l^+ l^-$ . The complete computations of NLL and NNLL precision of the decay for small dilepton mass can be found in [9] and [10], respectively. Recently, the first calculation of the NNLL contributions for arbitrary dilepton invariant mass is also available<sup>[11]</sup>. For consistency, we use NLL prediction<sup>[9]</sup> in our calculation, and exclude the resonances  $J/\psi$ ,  $\psi'$  contributions by using the same cuts as experiments<sup>[5]</sup> so we can compare our prediction with experiments. In addition, we also consider theoretical errors which come mainly from the uncertainties of  $m_t, m_b$  and  $m_c/m_b$ <sup>[8]</sup>, then combine the experimental and theoretical relative errors together.

Using the current average value for  $B \rightarrow X_s l^+ l^-$ <sup>[12]</sup>

$$\mathcal{B}r^{ex}(B \rightarrow X_s l^+ l^-) = (6.2 \pm 1.1_{-1.3}^{+1.6}) \times 10^{-6}, \quad (13)$$

in Fig. 3 we display the corresponding  $2\sigma$  experimental bounds on the size of  $z_{sb}$  and phase  $\theta$ . From this figure, we obtain

$$|z_{sb}| \leq 1.40 \times 10^{-3} \quad (95\% \text{ C.L.}). \quad (14)$$

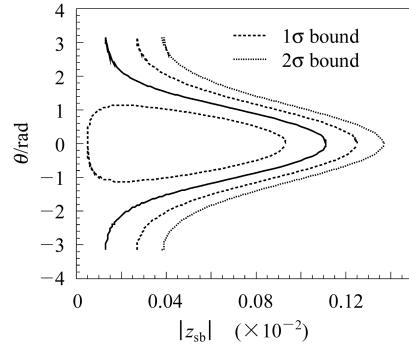


Fig. 3. The  $(|z_{sb}|, \theta)$  contour in Scenario A constrained by  $\mathcal{B}r^{ex}(B \rightarrow X_s l^+ l^-)$ . The dashed, dotted lines correspond to  $1\sigma$  and  $2\sigma$  experimental bounds of  $B \rightarrow X_s l^+ l^-$  in (13), respectively. The solid line denotes the experimental central value  $6.2 \times 10^{-6}$ . The region between dot lines is allowed at  $1\sigma$  level.

Now we turn to study the correlation of the branching ratios of  $B \rightarrow X_s \gamma$ <sup>[13]</sup> and  $B \rightarrow X_s l^+ l^-$  predicted in VQM. Our numerical result shows that (1)  $\mathcal{B}r(B \rightarrow X_s \gamma)$  is not so sensitive to the phase, which is not the case for  $\mathcal{B}r(B \rightarrow X_s l^+ l^-)$  as stated earlier; (2) within the experimental bounds of  $B \rightarrow X_s l^+ l^-$ , the corresponding branching ratio of  $B \rightarrow X_s \gamma$  predicted in VQM is consistent with the current average of the CLEO<sup>[14]</sup> and Belle<sup>[15]</sup> measurements

$$\mathcal{B}r^{ex}(B \rightarrow X_s \gamma) = (3.3 \pm 0.4) \times 10^{-4}. \quad (15)$$

It is very interesting to analyze how the zero of the forward-backward (FB) asymmetry ( $s_0$ ) is modified in VQM which is determined by equation

$$\text{Re}[(s_0 \mathcal{C}_9^{eff} + 2\mathcal{C}_{\gamma}^{eff}) \mathcal{C}_{10}^{eff*}] = 0. \quad (16)$$

Unlike the case of SM where  $\mathcal{C}_{10}^{eff}$  is real, the coefficient  $\mathcal{C}_{10}^{eff}$  is complex generally in VQM. Furthermore, the contributions to  $\mathcal{C}_{9,10}^{eff}$  from tree level FCNC diagram

$$|\mathcal{C}_{10}^{new}| \gg |\mathcal{C}_9^{new}|, \quad (17)$$

and subject to the constraints on  $z_{sb}$  from  $B \rightarrow X_s l^+ l^-$ ,  $|\mathcal{C}_{10}^{new}|$  still can be larger  $|\mathcal{C}_{10}^{SM}|$ , indicating that  $\mathcal{C}_{10}^{eff}$  can have large imaginary part. Therefore,  $s_0$  in VQM will have large deviation from that in SM.

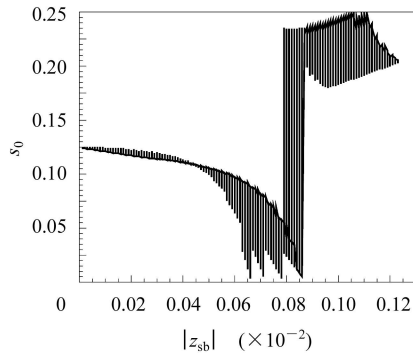


Fig. 4. The  $(|z_{sb}|, s_0)$  contour in VQM subject to the  $1\sigma$  bounds of  $\mathcal{B}v^{\text{ex}}(B \rightarrow X_s l^+ l^-)$ . For specified  $|z_{sb}|$ , the phase  $\theta$  effect on  $s_0$  is also shown.

Fig. 4 indicates that, subject to the experimental

measurement for branching ratio of  $B \rightarrow X_s l^+ l^-$ , the zero point of FB asymmetry is very sensitive to the parameters  $z_{sb}$  and phase  $\theta$ , especially in the region  $0.6 \times 10^{-3} < |z_{sb}| < 1.2 \times 10^{-3}$ .

Considering that the B factories such as BaBar and Belle are running, measurements for inclusive and exclusive B decays with high precision are expected. Therefore, the VQM will be tested in the near future.

*We would like to thank Profs. T. Morumzi, Y.Y. Keum, T. Yoshikawa and C.D. Lü for useful discussions.*

## References

- XIONG Z H, YANG J M. Nucl. Phys., 2001, **B602**: 289—306; Nucl. Phys., 2002, **B628**: 193—216; XIONG Z H, CHEN H S, LU L. Nucl. Phys., 1999, **B561**: 3—16; LU G R, XIONG Z H, CAO Y G. Nucl. Phys., 1997, **B487**: 43—54
- CHANG C-H V, CHANG D, Keung W Y. Phys. Rev., 2000, **D61**: 053007; Handoko L T, Morozumi T. Mod. Phys. Lett., 1995, **A10**: 309—322
- Ahmady M R, Nagashima M, Sugamoto A. Phys. Rev., 2001, **D64**: 054011; Barenboim G, Botella F G, Vives O. Nucl. Phys., 2001, **B613**: 285—305; Hawkins D, Silverman D. Phys. Rev., 2002, **D66**: 016008; Yanir T. JHEP, 2002, **0206**: 044
- Aubert B et al (BaBar Collaboration). hep-ph/0308016
- Kaneko J et al (Belle Collaboration). Phys. Rev. Lett., 2003, **90**: 021801
- Cho P, Grinstein B. Nucl. Phys., 1991, **B365**: 279—311;
- GAO C S, HU J L, LÜ C D et al. Phys. Rev., 1995, **D52**: 3978—3985
- Buchalla G, Buras A, Lautenbacher M E. Rev. Mod. Phys., 1996, **68**: 1125—1244
- Eidelman S et al (Particle Data Group). Phys. Lett., 2004, **592**: 1—1109
- Misiak M. Nucl. Phys., 1993, **B393**: 23—45
- Bobeth C, Misiak M, Urban J. Nucl. Phys., 2000, **B574**: 291—330; Asatrian H H, Asatrain H M, Greub C et al. Phys. Rev., 2002, **D65**: 074004; Phys. Lett., 2001, **B507**: 162—172
- Ghinculov A, Hurth T, Isidori et al. Nucl. Phys., 2004, **B685**: 351—392
- Nakao M. Int. J. Mod. Phys., 2004, **A19**: 934—948
- Chetyrkin K, Misiak M, Munz M. Phys. Lett., 1997, **B400**: 206—219
- CELO Collaboration, CHEN S et al. Phys. Rev. Lett., 2001, **87**: 251807
- Abe K et al. Phys. Lett., 2001, **B511**: 151—158

## B 稀有辐射衰变对似矢量夸克模型约束的研究

熊兆华<sup>1)</sup>

(北京工业大学应用数理学院理论物理室 北京 100022)

**摘要** 在似矢量夸克模型中, 具有一个为  $SU(2)$  单态的下夸克  $D$  以及树图  $b \rightarrow sZ^*$  相互作用  $z_{sb}$ . 在此框架下, (1) 通过考察描述  $B \rightarrow X_s \gamma$  的 Wilson 系数随重正化标度从  $m_D$  到弱标度的跑动, 研究了  $D$  夸克对此衰变的影响. (2) 使用最近对  $B \rightarrow X_s l^+ l^-$  的测量, 获得了对  $z_{sb}$  相当严格的限制. 发现前后不对称的零点值可以与标致模型的预言有大的偏离, 并对  $z_{sb}$  十分敏感, 可以用来探测新物理.

**关键词** B 稀有辐射衰变 树图相互作用  $bsZ$  似矢量夸克模型

2005 - 08 - 15 收稿, 2005 - 10 - 26 收修改稿

1) E-mail: xiongzh@mail.ihep.ac.cn